Algorithm Description for the TEMPO Total Ozone Retrieval Algorithm

Junsung Park[1], Xiong Liu[1], John Houck[1], Dave Haffner[2,3], Kelly Chance[1]

[1]Smithsonian Astrophysical Observatory

[2]NASA Goddard Space Flight Center

[3]Science Systems and Applications Inc. (SSAI)

Corresponding author: Junsung Park (joonsung.park@cfa.harvard.edu)

Key Points:

- As the TEMPO total ozone algorithm is adapted from the OMI TOMS V8.5 total ozone algorithm, this document provides a brief description of the algorithm and the details about the modifications for TEMPO. More information about the TOMS algorithm can be found in the OMI algorithm theoretical basis document for ozone products, chapter 2.
- Preliminary evaluation of the V04 TEMPO O3TOT product and describes the known issue of the V04.

Version: 2.2

Release Date: February 23, 2026

DOI: 10.5067/doc/tempo/AlgorithmDescription_L2-3/o3tot/V2.2

Abstract

For the Tropospheric Emissions: Monitoring of Pollution (TEMPO), the OMTO3 V8.5 (also known as Total Ozone Mapping Spectrometer (TOMS) V8.5) algorithm has been adapted to retrieve total ozone columns. The TEMPO Total Ozone algorithm uses two wavelength pairs, one (317.62 nm for Ozone and 331.34 nm for the reflectivity) is for most conditions, and the other (331.34 and 360.15 nm) is for high ozone and high solar zenith angle conditions. For adapting to the TEMPO, four parts have been updated: first is expanding viewing geometry to accommodate TEMPO's larger observing viewing zenith angle (VZA), second is an updated Look-Up Table (LUT) using TEMPO's on-orbit measured slit functions and the BDM (Daumont et al., 1922; Brion et al., 1993; Malicet et al., 1995) ozone absorption cross sections, third is using optical centroid cloud pressure from the TEMPO cloud (CLDO4) product, and fourth is performing additional soft calibrations. The main product parameters are total column ozone (TCO) and ultraviolet aerosol index (UVAI) for the TEMPO at each native spatial pixel.

Plain Language Summary

Ozone has a profound influence on the atmosphere and life on Earth. The ozone layer in the stratosphere acts as a protector of the Earth's life from harmful solar ultraviolet radiation and constitutes ~90% of the total ozone. It is an important greenhouse gas in the upper troposphere and lower stratosphere and plays a very important role in tropospheric chemistry in the troposphere. It is a major pollutant and toxic to biota near the surface. So, it is essential to monitor both total ozone and its vertical distribution due to its key roles in different parts of the atmosphere. TEMPO (Tropospheric Emissions: Monitoring of Pollution) is a satellite mission in geostationary orbit used for measuring trace gases and aerosols of importance to air quality over North America. This document describes the retrieval algorithm and product details for the TEMPO total ozone product.

Keywords: TEMPO, Total Ozone, UV aerosol index

Version Description

This is Version 2.2 of the algorithm description for the TEMPO Level 2 total ozone retrieval algorithm.

1 Introduction

TEMPO is NASA's first Earth Venture Instrument (EVI-1) project, selected in 2012 (Zoogman et al., 2017). It is a PI-led instrument project at the Smithsonian Astrophysical Observatory (SAO) with project management at NASA Langley Research Center (LaRC) and instrument development at Ball Aerospace. TEMPO is NASA's first host payload. NASA LaRC was designated to manage the mission project to find the satellite provider and host and launch for TEMPO. After the TEMPO instrument delivery in November 2018, the TEMPO mission joined with the satellite provider Maxar in 2019 and the host IntelSat in 2020. The TEMPO instrument will launch on board the commercial geostationary communication satellite IntelSat-40e (IS-40e) via SpaceX Falcon 9 into a geostationary orbit at 91°W.

TEMPO uses the UV/visible spectroscopic technique to measure atmospheric pollution across North America, from Mexico City/Puerto Rico to the Canadian oil sands, and from the Atlantic to the Pacific, hourly and at high spatial resolution. TEMPO spectroscopic measurements in the ultraviolet and visible wavelengths provide a tropospheric measurement suite that includes the key gases of tropospheric air pollution chemistry. Measurements are made from geostationary orbit for nearly continuous daylight monitoring and to capture the inherent high variability in the diurnal cycle of emissions and chemistry. A small spatial footprint resolves pollution sources at a sub-urban scale. Together, high temporal and spatial resolution improves emission inventories, better monitors population exposure, and enables effective emission-control strategies.

The detailed descriptions of the TEMPO instrument and measurements are described in the previous study (Zoogman et al., 2017) and TEMPO L0-1 ATBD (Chong et al. 2026).

1.1 Scope of this ATBD

The purpose of this algorithm description document is to describe the TEMPO total ozone retrieval algorithm (TEMPO O3TOT) briefly. This TEMPO O3TOT algorithm is based on the TOMS V8.5 algorithm, and the detailed descriptions are in the OMI algorithm theoretical basis document (ATBD) for ozone products (https://ozoneaq.gsfc.nasa.gov/content/public/OMI/ATBDs/ATBD-OMI-02.pdf, chapter 2). The generated output contains the retrieved total ozone, SO_2 index, and UV aerosol index. It contains ozone columns below the cloud, effective cloud fraction, radiative cloud fraction, cloud pressure, surface reflectivity at 331 nm, surface refractivity at 360 nm, terrain height, and terrain pressure. The quality flag and algorithm are very useful parameters for evaluating a retrieved total ozone. The detailed evaluation of the TEMPO O3TOT products and known issues are described in TEMPO Total Ozone Level 2 and 3 Data product: User Guide (Park et al., 2026).

2 Algorithm Description

The TOMS algorithm is based on theoretical work developed by Dave and Mateer in 1967, making it a foundational concept in the field of atmospheric science for almost half a century. This algorithm uses two wavelengths (317.5 and 331.2 nm) to estimate the Total Column Ozone (TCO) based on BUV radiances from satellite observation. This TOMS algorithm was adapted to the TEMPO total ozone (O3TOT) algorithm.

The TEMPO algorithm uses two wavelength pairs, one is 317.62 and 331.34 nm under most conditions, the other is 331.34 and 360.15 nm for high ozone and high solar zenith angle conditions. The longer of the two wavelengths is used to derive effective cloud fraction (f_c) based on the Mixed Lambert Equivalent Reflectivity (MLER) model that was developed to model the effect of clouds on Rayleigh scattering. In this MLER model, the scene consists of a clear-sky scene of surface reflectivity of 0.15 and a cloudy scene of cloud reflectivity of 0.8 based on the independent pixel approximation:

$$I = I_{clr} \times (1 - f_c) + I_{cld} \times f_c \quad (1)$$

where I, I_{clr} and I_{cld} are the overall, clear, and cloudy scene radiances, respectively. When f_c becomes less than zero or when there is snow/ice, we assume that no cloud is present and use the Lambert Equivalent Reflectivity (LER) model to derive the clear scene reflectivity R. When f_c exceeds 1, we assume 100% cloud cover and derive cloud reflectivity using the LER model. Given the derivation of f_c and/or R from the longer wavelength, the shorter (stronger ozone-absorbing) wavelength is used to derive total ozone. The effective cloud-top pressure is taken from the retrieved Optical Cloud Centroid Pressure (OCCP) inferred from the newly implemented TEMPO O_2-O_2 cloud algorithm when available. Otherwise, it is taken from the climatological Optical Cloud Centroid Pressure (OCCP) from the OMCLDRR product. In either the MLER or LER model, the retrieved ozone column is the weighted ozone column above surface and OCCP by Cloud Radiative Fraction (CRF), defined as $f_c \times I_{cld} \div I$. To estimate the total column amount, the "un-measured" or ghost column below OCCP (also weighted by CRF) is estimated using an ozone climatology and added to the retrieved ozone column.

The algorithm also derives the absorbing aerosols by calculating the radiance residual at 360.15 nm. The absorbing Aerosol Index (AI) is defined as the logarithmic contrast between

measured and Rayleigh-calculated radiances at 360.15 and 331.34 nm. Reflectivity derived at 331.34 nm is used to compute the expected radiance at 360.15 nm under a Rayleigh-only atmosphere using precomputed lookup tables. Positive AI values indicate the presence of UV-absorbing aerosols. The AI is useful for tracking global transport of smoke and dust, for it can track these aerosols above and through clouds, as well as over snow/ice covered surfaces. Various studies have indicated that AI is very nearly proportional to the aerosol absorption optical depth at 360 nm. However, the proportionality constant varies with the altitude (of the center of mass) of the aerosol layer, the lower the altitude the smaller the constant. Most aerosols have stronger absorption in the UV than in the visible, including mineral dust from deserts and carbonaceous aerosols containing organic and black carbon. Since the AI is also affected by the spectral dependence of surface albedo caused by sea-glint and water–leaving radiance, and since there are residual errors in the MLER model in estimating Rayleigh scattering in presence of clouds, we recommend that only the AI values larger than +1 should be used for aerosol studies and areas contaminated by sea-glint should be avoided completely. Since absorbing aerosols causes the ozone derived from the basic ozone retrieval algorithm to be overestimated, a parametric relationship based on AI is used to correct the initial retrieved ozone column. This relationship also appears to remove a large portion of errors caused by sea-glint. Other than the three primary wavelengths mentioned above, the total ozone algorithm uses additional wavelengths for quality control and error correction in more restricted geophysical situations. These include correction for ozone profile shape errors at large solar zenith angles using 312.62 nm measurements, and the detection of strong sulfur-dioxide contamination using multiple wavelength pairs. For a more detailed description of the algorithm please refer to the Algorithm Theoretical Basis Document (ATBD) at https://ozoneaq.gsfc.nasa.gov/content/public/OMI/ATBDs/ATBD-OMI-02.pdf, chapter 2.

The total ozone algorithm is one of the two algorithms that derive total ozone values from TEMPO. It performs retrieval at the native spatial resolution. The other is the ozone profile algorithm based on the optimal estimation approach. It takes advantage of TEMPO's hyperspectral measurements and can retrieve more vertical information from TEMPO radiance spectrum in the UV and visible. Therefore, it can potentially be more accurate. However, due to the involvement of on-line radiative transfer calculation, the ozone profile retrieval is very slow and is only

performed on aggregated pixels (4 native spatial pixels coadded; currently 4 pixels across the track or in the N/S direction are).

2.1 Atmospheric Model and Trace Gas Profiles

The TEMPO O3TOT algorithm mainly uses atmospheric trace gas profiles and meteorological parameters from the TOMS V8 climatology data as shown in Table 1.

Table 1. *Ancillary data used in the TEMPO O3TOT algorithm.*

Input	Source
Cloud-top pressure	TEMPO CLDO4 product Defaults to cloud pressure climatology (OMI-derived) if cloud retrieval is unavailable.
Cloud fraction	Retrieved based on the MLER. If $f_c \leq 0$ or ≥ 1, it is set to 0 or 1, R_s or R_{cld} is retrieved instead.
Ozone profiles	TOMS V8 climatology (total ozone dependent, monthly / 10° zonally averaged)
Temperature profiles	TOMS V8 climatology (monthly / 10° zonally averaged)
Surface albedo	15% or directly retrieved as R_s if $f_c = 0$
Snow/ice fraction	Climatology at 1° × 1° from the TOMS V8
Terrain height pressure	Climatology at 1/3° × 1/3° from the TOMS V8
Aerosols	Not explicitly treated, but an aerosol correction is included

2.2 Quality Flags

TEMPO O3TOT product has two quality flags, one is algorithm_flags in support_data group reports the overall quality of the retrieval, the other is quality_flag in product_group reports the detailed quality of the retrieval.

Detailed descriptions for algorithm flag and quality flag are shown in Table 2 and Table 3, respectively.

Table 2. *Algorithm flags in the TEMPO O3TOT product.*

Value	Descriptions

0	Skipped
1	Standard
2	Adjusted for profile shape
3	Based on C-pair (331 and 360 nm)
10	Snow/Ice

Table 3. *Quality flags in the TEMPO O3TOT product.*

Value	**Descriptions**
Bits 0 to 3 together contain several output error flags (Note in the case of multiple error flags, only the highest error flag is reported.)	
0	Good sample
1	Glint contamination (corrected)
2	SZA > 84°
3	360 residual > threshold
4	Residual at unused ozone wavelength > 4 sigma
5	SOI > 4 sigma (SO_2 present)
6	Non-convergence
7	Abs (residual) > 16.0 (fatal)
8	Row anomaly error (same as bit 6 in this field)
Bits 4 to 5 are reserved for future use (currently set to 0)	
Bit 7 is set to 0 when TEMPO CLDO4 cloud pressure is used and set to 1 when climatological cloud pressure is used	
Bits 8 to 15 are flags that are set to 0 for FALSE (good value), or 1 for TRUE (bad value)	
Bit 8	Geolocation error (anomalous FOV Earth location)
Bit 9	SZA > 88°
Bit 10	Missing input radiance
Bit 11	Error input radiance

Bit 12	Warning input radiance
Bit 13	Missing input irradiance
Bit 14	Error input irradiance
Bit 15	Warning input irradiance

2.3 Algorithm Output Variables

Table 4 presents key variables in the TEMPO L2 O3TOT product file.

Table 4. *Key variables in the TEMPO L2 O3TOT product file.*

Name	Long name	Unit
/product/column_amount_o3	Column amount o3	DU
/product/fc	fc	-
product/ o3_below_cloud	o3 below cloud	DU
/product/quality_flag	quality flag	-
/product/radiative_cloud_frac	radiative cloud frac	-
/product/so2_index	so2 index	-
/product/uv_aerosol_index	uv aerosol index	-
/support_data/a_priori_layer_o3	a priori layer o3	DU
/support_data/algorithm_flags	algorithm flags	-
/support_data/cloud_pressure	cloud pressure	hPa
/support_data/lut_wavelength	lut wavelength	nm
/support_data/step1_o3	step1 o3	DU
/support_data/step2_o3	step2 o3	DU
/support_data/surface_reflectivity_at_331nm	surface reflectivity at 331nm	percent
/support_data/suface_reflectivity_at_360nm	surface reflectivity at 360nm	percent
/support_data/terrain_height	terrain height	m

/support_data/terrain_pressure	terrain pressure	hPa

3 TEMPO O3TOT updates history

This section describes updates to the TEMPO O3TOT algorithm.

3.1 Version 04 TEMPO O3TOT Updates and Status

3.1.1 Look-up table update

In the V3 O3TOT data product, look-up tables were built using BDM cross sections convolved with a triangular slit function with a full width at half maximum of 0.60 nm. For V4, we updated the look-up tables by using BDM cross sections with on-orbit slit functions (assuming asymmetric super Gaussian) from first light, averaged over all spatial pixels for each of 12 wavelengths in the look-up tables. The look-up tables were corrected for the Ring effect, also with the same cross sections (Fig. 1).

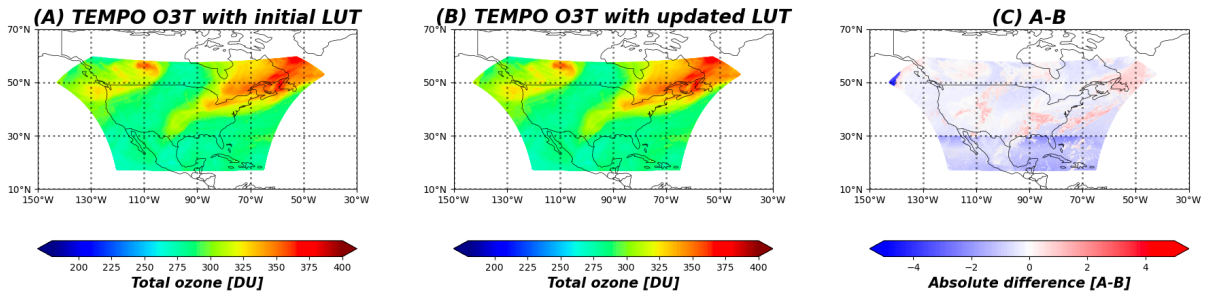

Figure 1. *Effect of the Look-Up Table (LUT) updates on total column ozone retrieval on July 26, 2025. (left) Retrieval using the updated V04 TEMPO O3TOT algorithm with the initial LUT used in the V03 TEMPO O3TOT algorithm. (middle) Retrieved using the updated V04 TEMPO O3TOT algorithm with the updated LUT used in the V04 TEMPO O3TOT algorithm. (right) Absolute difference between (A) and (B).*

3.1.2. Soft calibration

After a systematic reduction of the normalized radiance by ~13.4% in the UV band in V04 L1 data, we applied additional soft calibration to the irradiance at wavelengths of 312.61 nm, 317.62 nm, and 360.15 nm. The values of 0.966, 0.969, and 0.99 have been used as soft calibration factors for 312.61 nm, 317.62 nm, and 360.15 nm, respectively. The Fig. 2 and 3 below show the comparison between total column ozone from the TEMPO O3TOT product and the OMPS NPP O3TOT product. Before the soft calibration, the TEMPO O3TOT product had a significant latitude-dependent bias (Fig. 2) of about 3% high bias over low latitudes and 2% low bias over high latitudes (Zhao et al., 2025), while after this soft calibration, the TEMPO O3TOT

product shows improvement in the latitude-dependent bias (Fig. 3). The V04 L1b update and this soft calibration not only improve the total ozone but also remove the systematic negative bias of ~-2 in the UV aerosol index (Fig. 4).

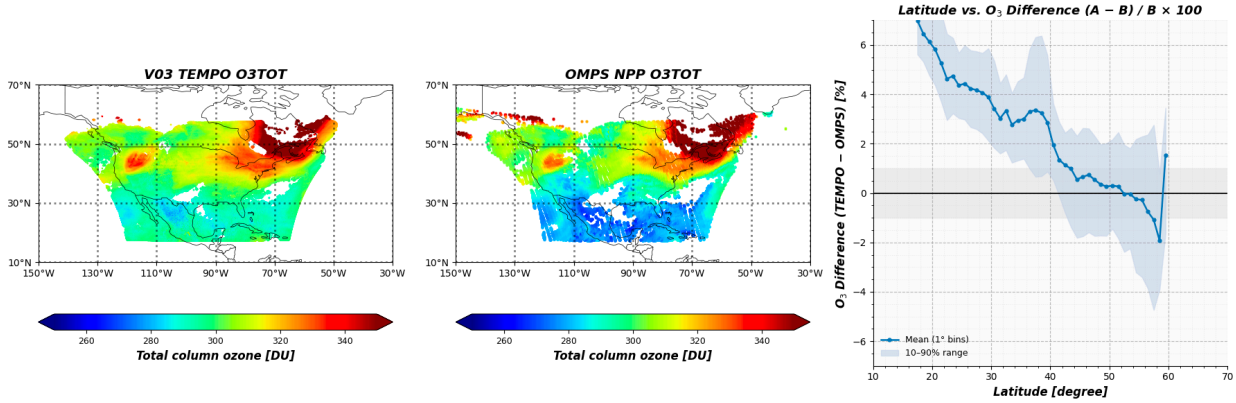

Figure 2. *Comparison between total column ozone from the V03 TEMPO O3TOT product and the OMPS NPP O3TOT product. (left) Spatial distribution of the total column ozone from the V03 TEMPO O3TOT product on September 03, 2024 (S008). (middle) Spatial distribution of the total column ozone from the OMPS NPP product on September 03, 2024 (S008). (right) Relative difference between TEMPO and OMPS NPP as a function of wavelength.*

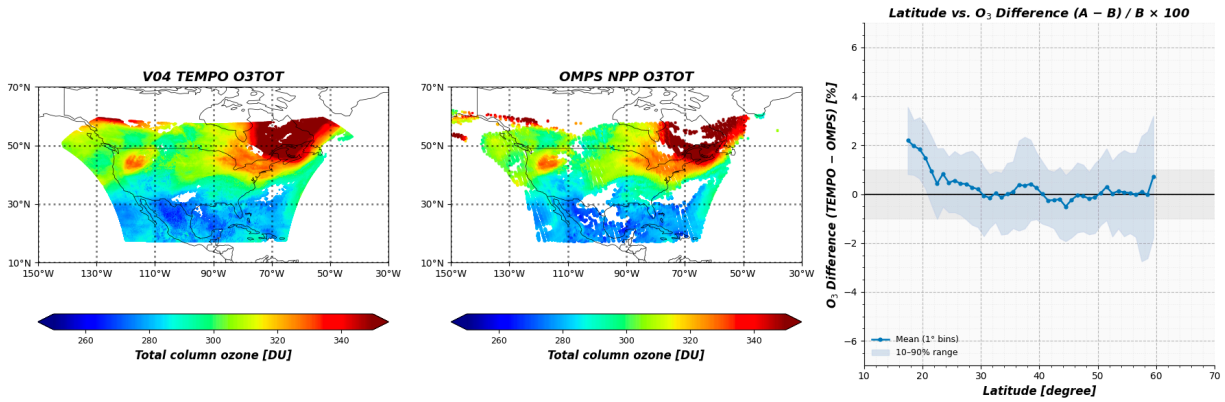

Figure 3. *Comparison between total column ozone from the V04 TEMPO O3TOT product and the OMPS NPP O3TOT product. (left) Spatial distribution of the total column ozone from the V04 TEMPO O3TOT product on September 03, 2024 (S008). (middle) Spatial distribution of the total column ozone from the OMPS NPP product on September 03, 2024 (S008). (right) Relative difference between TEMPO and OMPS NPP as a function of wavelength.*

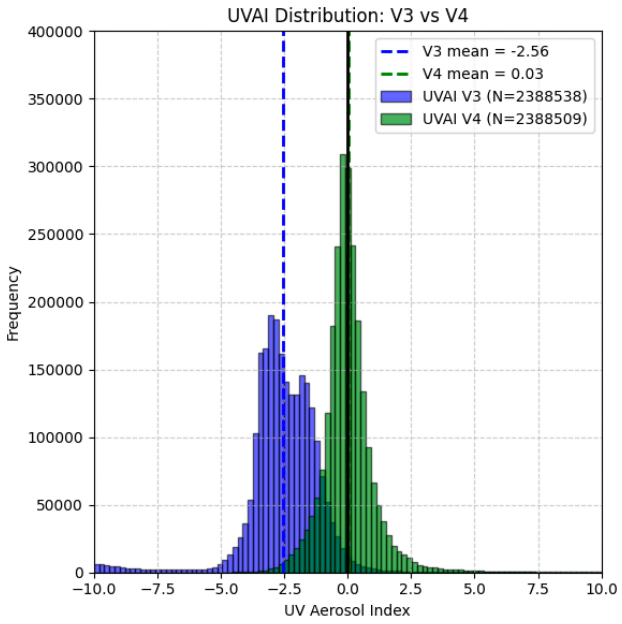

Figure 4. *Comparison of the UVAI in the TEMPO O3TOT product for the same scan on September 3, 2024. Blue and green bars represent the UVAI from V03 TEMPO O3TOT and V04 TEMPO O3TOT, respectively. Blue and green dashed lines represent the mean value of each UVAI.*

3.1.3. Quality flag

The "quality_flag" variable in the product group of the L2 file provides detailed information on the retrieval quality. In V04 TEMPO O3TOT, this variable did not function as intended (see Fig. 5A). For V04, the ascending and descending flag was removed, and a sun-glint possibility flag was added. With these updates, "quality_flag" now provides the information correctly (Fig. 5B).

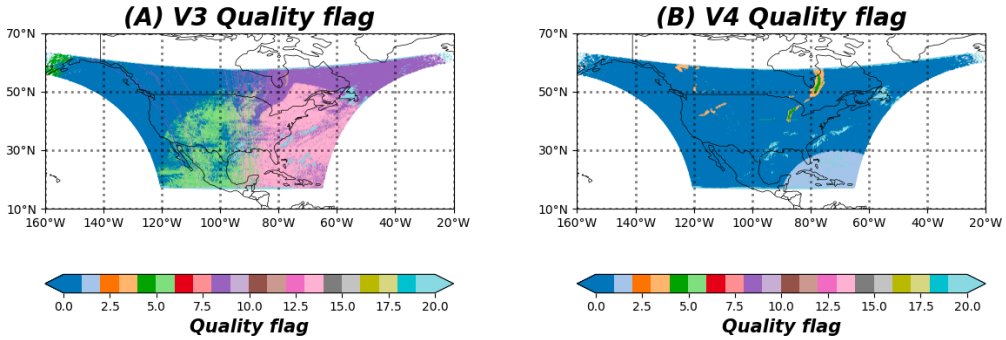

Figure 5. *Comparison of the quality flag in the TEMPO O3TOT product for the same scan: V03 (left) and V04 (right).*

3.1.4. Evaluation of V04 TEMPO O3TOT product

The detailed explanations and results will be submitted as a TEMPO total column ozone paper soon. The publicly released V04 TEMPO O3TOT product was evaluated using ground-based Pandora observations from the Pandonia Global Network (PGN). Co-location criteria of ±15 minutes and 5 km in horizontal distance were applied. Only high-quality total column ozone measurements from both TEMPO and Pandora were included in this comparison based on the following filtering criteria:

- TEMPO
    1) Cloud fraction (CF) ≤ 0.5
    2) Solar zenith angle (SZA) ≤ 80º
    3) Viewing zenith angle (VZA) ≤80º
    4) Quality flag = 0
- Pandora
    1) Quality flag = 0 & 10

The Pandora observation sites included in this comparison, after application of the above quality filtering, are shown in Figure 6.

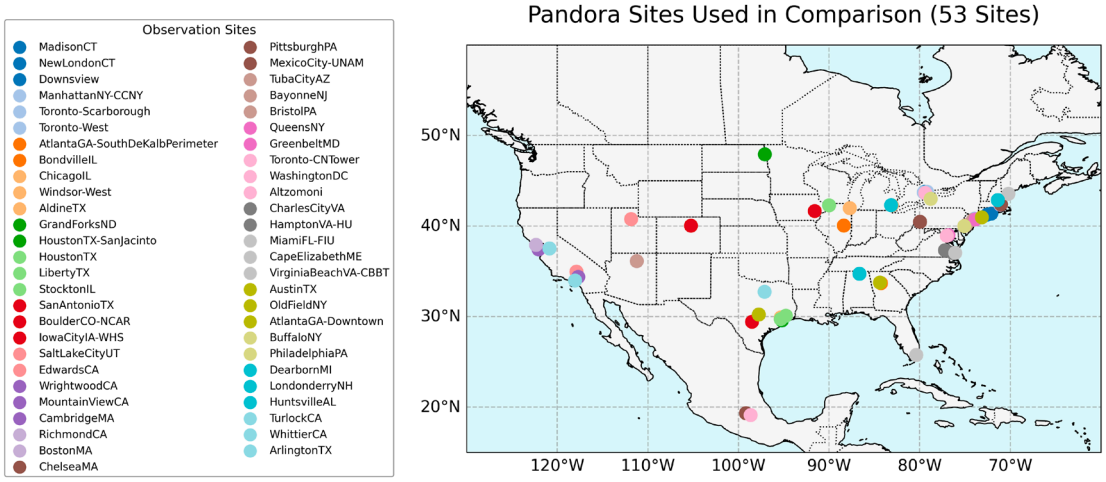

Figure 6. *Locations of Pandora observation sites used for comparison with TEMPO observations.*

Total column ozone retrieved from TEMPO observations shows a good agreement with co-located Pandora measurements. An analysis of 10,547 coincident observations shows a high

correlation coefficient (R = 0.98) between TEMPO and Pandora total column ozone. The mean bias is -2.13% with a root mean square error of 2.72% (top row in Figure 7).

Time-series comparisons from September to December 2025 demonstrate stable overall performance, with no significant dependence at the daily scale as shown in Figure 7. However, in the monthly-averaged comparison (bottom row in Figure 7), a negative bias increases from September to December. This month-to-month increase in negative bias is associated with progressively higher solar and viewing zenith angles (SZA and VZA).

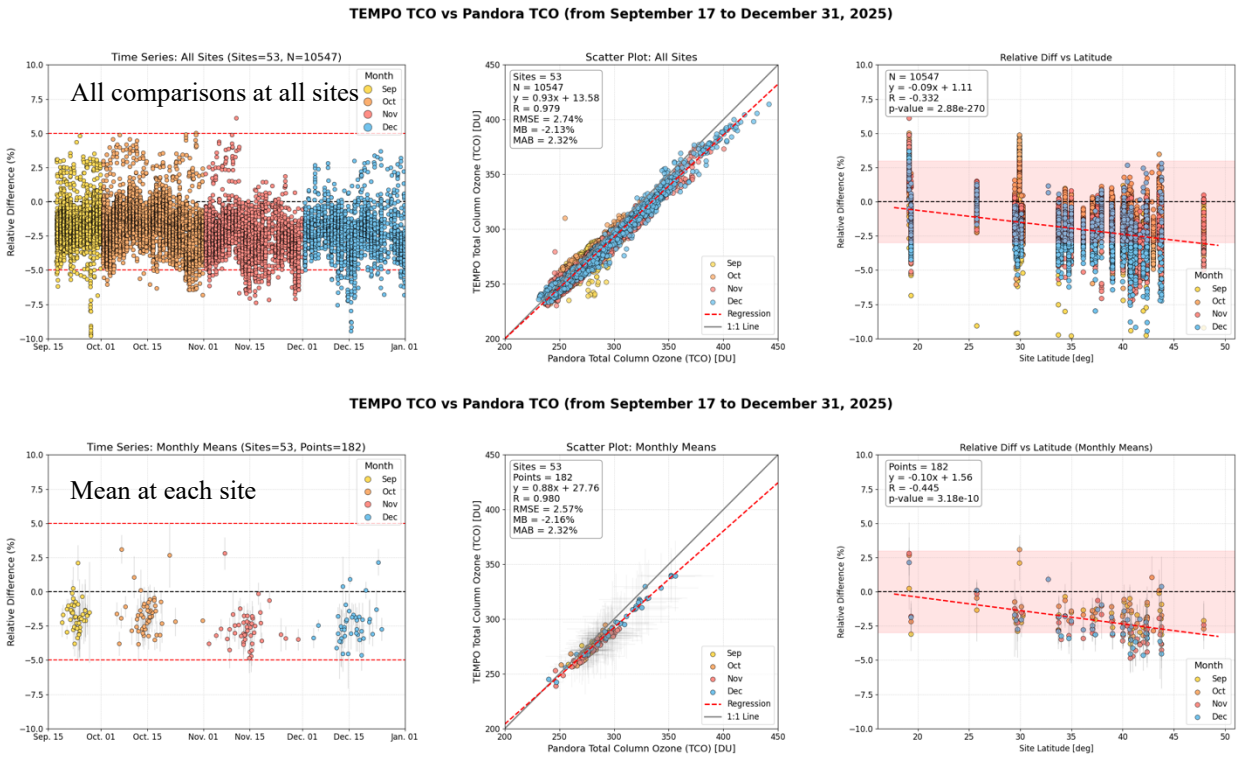

Figure 7. *Total column ozone comparison between V04 TEMPO O3TOT and Pandora measurements. The top row shows comparisons for all individual coincident observations across all Pandora sites, while the bottom row shows comparisons based on monthly averages at each site. The left, middle, and right columns display the time series of relative differences, the correlation analysis, and the relative difference as a function of latitude, respectively. Different colors indicate different months.*

In addition, the known issue of latitudinal-dependent bias has improved compared to V03, which exhibited a strong latitudinal gradient (Slope: -0.124) and large positive bias at low latitudes (approximately +3%). In the current V04, the low-latitude positive bias has been effectively mitigated, although a small negative bias (~-1%) persists, as shown in Figure 8.

Furthermore, as shown in Figures 8 and 9, the negative bias increases at large geometric angles (i.e., high SZA and VZA). In Figure 8, TEMPO TCO demonstrates an excellent agreement with OMPS NPP TCO over all latitudes within 1% of absolute mean bias (August 2023), while in Figure 9, TEMPO TCO demonstrates an increase in the absolute mean bias at high latitudes due to the high solar and viewing zenith angle in winter (December 2024). In future algorithm updates, these issues should be addressed by optimizing the C-pair selection and profile-shape switching threshold using the expanded TEMPO observation dataset.

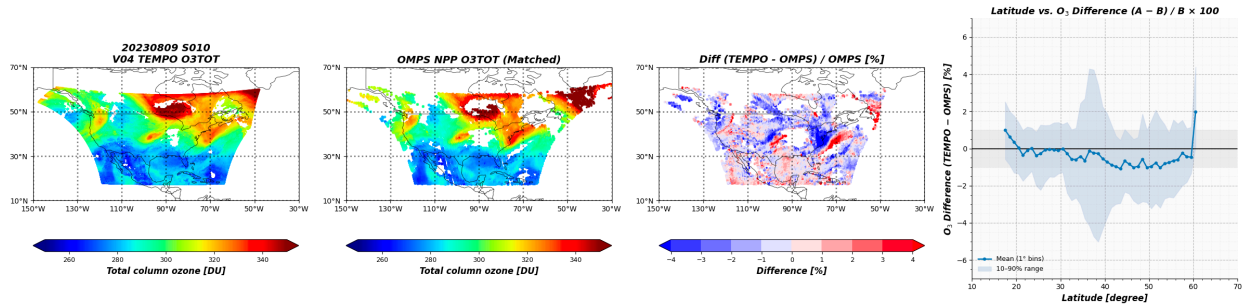

Figure 8. *Total column ozone (TCO) comparison between TEMPO and OMPS NPP on August 9, 2023. TEMPO TCO is based on operational V04 data, and OMPS NPP is based on V2.1.*

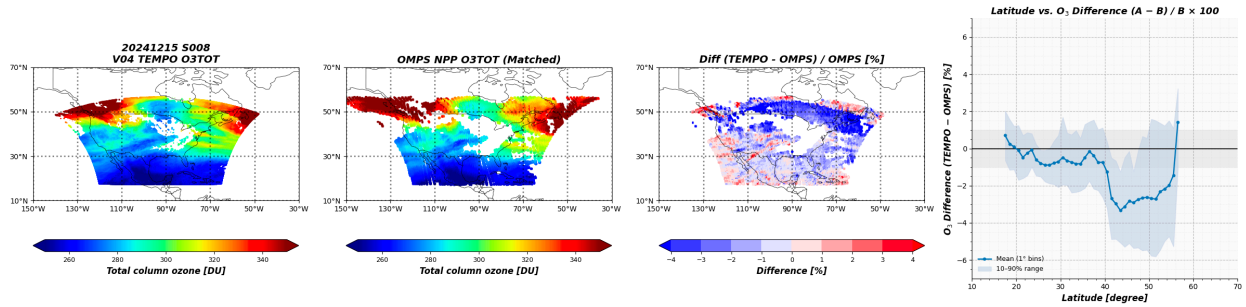

Figure 9. *Total column ozone (TCO) comparison between TEMPO and OMPS NPP on December 15, 2024. TEMPO TCO is based on operation V04 data, and OMPS NPP is based on V2.1.*

4 References

Bass, A. M., & Paur, R. J. (1985). The ultraviolet cross-sections of ozone: I. The measurements. In *Atmospheric Ozone: Proceedings of the Quadrennial Ozone Symposium held in Halkidiki, Greece 3–7 September 1984* (pp. 606-610). Dordrecht: Springer Netherlands. https://doi.org/10.1007/978-94-009-5313-0_120

Brion, J., Chakir, A., Daumont, D., Malicet, J., & Parisse, C. (1993). High-resolution laboratory absorption cross section of O3. Temperature effect. *Chemical physics letters*, *213*(5-6), 610-612. https://doi.org/10.1016/0009-2614(93)89169-I

Bhartia, P. K., & Wellemeyer, C. W. (2002). *TOMS-V8 total O3 algorithm. OMI Algorithm Theoretical Basis Document Volume II, NASA Goddard Space Flight Center Tech. Doc*. ATBD-OMI-02, 15–31, https://ozoneaq.gsfc.nasa.gov/content/public/OMI/ATBDs/ATBD-OMI-02.pdf

Chong, H., Liu, X., Houck, J., Flittner, D. E., Carr, J., Hou, W., Suleiman, R. M., & Chance, K. (2026). TEMPO Level 1 Data Product: User Guide. https://asdc.larc.nasa.gov/documents/tempo/guide/TEMPO_Level-1_user_guide_V2.0.pdf

Chong, H., Liu, X., Houck, J., Flittner, D. E., Carr, J., Hou, W., Davis, J. E., Suleiman, R. M., Chance, K., Mishra, N., Chan Miller, C., González Abad, G., Baker, B., Lasnik, J., Nicks, D., Bak, J., Nowlan, C. R., Wang, H., Park, J., O'Sullivan, E., Fitzmaurice, J., & Carpenter, L. (2026). Algorithm theoretical basis document for the TEMPO Level 0-1 processor. https://doi.org/10.1029/2025EA004516

Daumont, D., Brion, J., Charbonnier, J., & Malicet, J. (1992). Ozone UV spectroscopy I: Absorption cross-sections at room temperature. *Journal of Atmospheric Chemistry*, *15*, 145-155. https://doi.org/10.1007/BF00053756

Dave, J. V., & Mateer, C. L. (1967). A preliminary study on the possibility of estimating total atmospheric ozone from satellite measurements. *Journal of the Atmospheric Sciences*, *24*(4), 414-427. https://doi.org/10.1175/1520-0469(1967)024<0414:APSOTP>2.0.CO;2

Malicet, J., Daumont, D., Charbonnier, J., Parisse, C., Chakir, A., & Brion, J. (1995). Ozone UV spectroscopy. II. Absorption cross-sections and temperature dependence. *Journal of atmospheric chemistry*, *21*, 263-273. https://doi.org/10.1007/BF00696758

Park, J., Liu, X., Bak, J., Houck, J., Chance, K., Suleiman, R. M., Davis, J, E., Chong, H., Hou, W., Flittner, D. E., Carr, J., O'Sullivan, E., González Abad, G., Knowland, K. E., Chan Miller, C., Nowlan, C. R., Wang, H., Fitzmaurice, J., Carpenter, L., Spurr, R., & Newchurch, M. J. (2026). Algorithm theoretical basis document for the TEMPO Ozone Profile Retrieval Algorithm.

Park, J., Liu, X., Houck, J., Haffner, D., & Chance, K. (2026). TEMPO Total Ozone Level 2 and 3 Data product: User Guide.

Zhao, X., Griffin, D., Fioletov, V., McLinden, C., Liu, X., Park, J., Petropavlovskikh, I., Hanisco, T.F., Hanisco, T., Szykman, J., Valin, L., Baumann, E., Cede, A., Tiefengraber, M., Gebetsberger, M., Uesato, I., Zheng, X., Ahn, S., Chang, L., Lee, W., Kim, J., Lee, H., Baek, K., Redondas, A., Fujiwara, M., Wang, T., Grutter, M., Houck, J., Haffner, D., & Lee, S. (2025). Geostationary Satellites Total Ozone Observations: First Results on Ground-based Networks Validation Efforts for TEMPO and GEMS. *Geophysical Research Letters,* 52, e2025GL114768. https://doi.org/10.1029/2025GL114768

Zoogman, P., Liu, X., Suleiman, R. M., Pennington, W. F., Flittner, D. E., Al-Saadi, J. A., Hilton, B. B., Nicks, D. K., Newchurch, M. J., Carr, J. L. Janz, S. J., Andraschko, M. R., Arola, A., Baker, B. D., Canova, B. P., Chan Miller, C., Cohen, R. C., Davis, J. E., Dussault, M. E., Edwards, D. P., Fishman, J., Ghulam, A., González Abad, G., Grutter, M., Herman, J. R., Houck, J., Jacob, D. J., Joiner, J., Kerridge, B. J., Kim, J., Krotkov, N. A., Lamsal, L., Li, C., Lindfors, A., Martin, R. V., McElroy, C. T., McLinden, C., Natraj, V., Neil, D. O., Nowlan, C. R., O′Sullivan, E. J., Palmer, P. I., Pierce, R. B., Pippin, M. R., Saiz-Lopez, A., Spurr, R. J. D., Szykman, J. J., Torres, O., Veefkind, J. P., Veihelmann, B., Wang, H., Wang, J., & Chance, K. (2017). Tropospheric emissions: Monitoring of pollution (TEMPO). *Journal of Quantitative Spectroscopy and Radiative Transfer*, *186*, 17-39. https://doi.org/10.1016/j.jqsrt.2016.05.008